CERN ν

Neutrino Factory Note 19

March 27, 2000

Electron losses in the arcs of the muon storage ring

André Verdier

Keywords:

Summary

A sizable fraction of the electron created in the muon storage ring have an energy not far from that of the muons. Therefore a part of those electrons emitted in the straight sections can propagate along the section and get lost in the first elements of the arcs. The associated power loss is estimated to be substantially larger than that associated with the local muon decay in the first elements of the arcs. It is important to take this power into account in the design of the cooling of these elements in order to avoid hot spots in the arcs.

1 Introduction

In the muon storage ring, the decay electron carry one third of the muon beam energy and dissipate it in the beam surrounding. The beam energy can be estimated as follows. The minimum muon intensity requested by the experiments is about 10^{21} per year. The average muon intensity can be obtained from the yearly machine time. The SPS statistics can be used to estimate this number. Typically, in 1999, 2852 hours, i.e. 1.03×10^7s, were actually used for physics (4300h used for operation, 3415h planned for physics [1]). Therefore the requested intensity corresponds to about 10^{14} muons per second on average in the muon storage ring. The associated power is 0.8MW for a muon beam energy of 50GeV, one third of which goes to the decay electrons. Eventually, for a 2km ring, the density of the power dissipated in the ring is 133W/m, i.e. more than two order of magnitudes larger than that of LHC [2]. This implies that the arc magnets have to be designed with a warm bore to evacuate this large energy density at room temperature.

This simple estimation of the deposited power density is not sufficient as the losses are modulated by the arc optics [3]. **Even more important,** the electrons (or positrons, in what follows the word electron will be used for either electron or positron) emitted by the muon decay are emitted in the direction of the muon beam with a small opening, i.e. half of them are emitted within an angle of $1/\gamma_\mu$ [4]. The distribution in energy of the electron emitted at angles smaller $1/\gamma_\mu$ has a maximum close to the muon energy. Such electrons emitted in a straight section can pass through the section like muons, because the synchrotron loss in the quadrupoles is negligible, and are lost in the arc because they have a large momentum deviation and they emit synchrotron radiations while the muons do not.

The aim of this note is to give an estimate of the increase of the energy loss in some arc elements due to this process.

In the first section the distribution of the decay electrons is recalled. In section 2 the fraction of electrons emitted in the straight section and reaching the arc is estimated. In section 3 the transport mechanism is explained. In section 4 the procedure to identify the electrons lost in the arcs is explained. In the last section the additional power associated with these electrons and dissipated in the arc is deduced.

2 Distribution of the decay electrons

We consider an unpolarised muon circulating on the axis of a straight section of the muon storage ring. When this muon decays, the neutrinos and the electron are emitted isotropically in the centre of mass. It can be shown that the distribution function of the electron in energy is given in the centre of mass by [4] :

$$dn/dx = 2Nx^2(3-2x) \tag{1}$$

x being the ratio between the momentum of the electron in the centre of mass p_e and half the muon mass, with $0 \leq x \leq 1$. There is no other dependence on the coordinates because of the isotropy of the process. Applying the Lorenz transformations [5], we obtain the components of the electron momentum in the laboratory assuming $\beta_\mu = 1$:

$$p_\parallel/p_e = \gamma_\mu(1+\cos\theta) \quad and \quad p_\perp/p_e = \sin\theta, \tag{2}$$

θ being the emission angle in the centre of mass. The electron angle is then :

$$p_\perp/p_\parallel = \frac{\sin\theta}{\gamma_\mu(1+\cos\theta)} \tag{3}$$

The angles of the electrons able to cross the straight section is limited by the section acceptance which corresponds to a maximum angle of $0.3/\gamma_\mu$ (this acceptance is such that the muon beam emittance does contribute little to the opening of the neutrino beam). Consequently the value of the angle θ (the emission angle in the centre of mass) is comprised between 0 and 0.5829rad according to equation 3. This in turn restricts the possible maximum longitudinal electron momentum according to equation 2 to values comprised between the muon energy E_μ (for θ=0) and $0.9174 \times E_\mu$ (for θ=0.5829rad). Consequently the energy distribution in the laboratory of the electron emitted with θ=0 and θ=0.5829rad are not terribly different. This is confirmed by simulations of muon decays [6]. The distribution of electrons with angles comprised between 0 and $0.3/\gamma_\mu$ is shown on figure (2).

In order to simplify the subsequent discussion, we assume that the energy distribution in the laboratory of the electrons able to cross the straight section is given by formula (1) in which x is the ratio between the electron energy and the muon energy.

It is important to note that this distribution is substantially different from the distribution in energy of the electrons in the whole space, which has a maximum close to zero and an

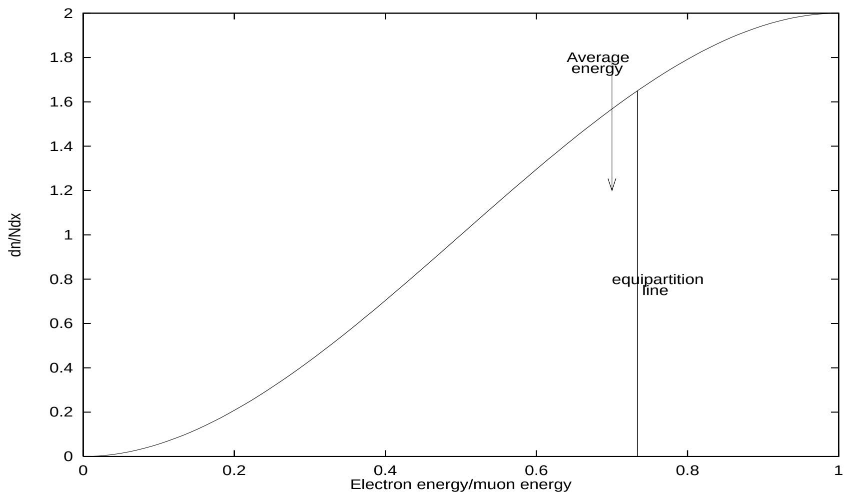

Figure 1: Distribution in energy of the electrons emitted with a small angle in the laboratory frame.

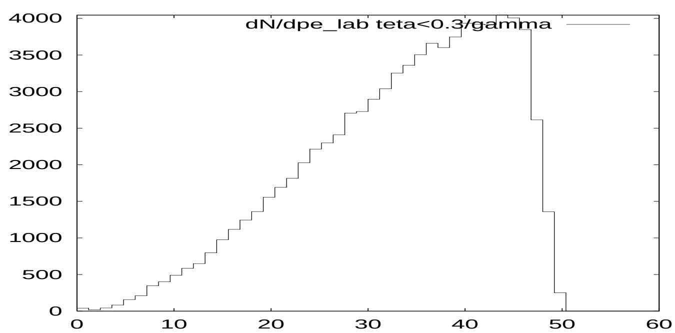

Figure 2: Distribution in energy of the electrons emitted in the laboratory frame with an angle comprised between 0 and $0.3/\gamma_\mu$ (simulation kindly done by J.B. Jeanneret).

average energy equal to one third of the muon energy [6]. This distribution is shown on figure (3).

Eventually we have to consider electrons emitted in the forward direction in a cone of maximum angle θ=0.5829rad in the centre of mass. This represents 8.26% = (1-cosθ)/2 of the total number of decay electrons, neglecting the electrons emitted backwards because they have a small energy (see formula 2). The actual number of electrons crossing the straight section is even less because of the transverse extension of the muon beam. This is examined next.

3 Electrons crossing the straight section

3.1 Energy acceptance of the straight section

The transverse acceptance of the storage ring is 3 r.m.s. beam size, in order to limit the loss of the injected muon beam to 1% (this is the truncation of a Gaussian distribution at 3σ).

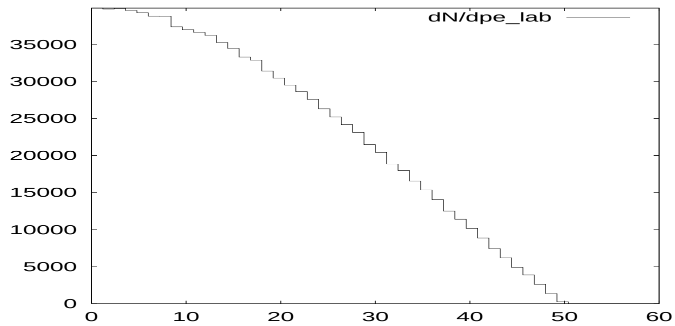

Figure 3: Distribution in energy of the decay electrons in the whole space (simulation kindly done by J.B. Jeanneret).

Several designs of storage rings have been produced (see for instance [7] and [8]). They all feature straight sections designed to make an r.m.s. beam divergence of $0.1/\gamma_\mu$ as mentioned above. These sections contain some FODO cells with a low phase advance. In the design [7] there are four cells which make a total length of about 500m. A more efficient ring could be made with a larger section of 800m [9], i.e. six cells, it will be considered in what follows.

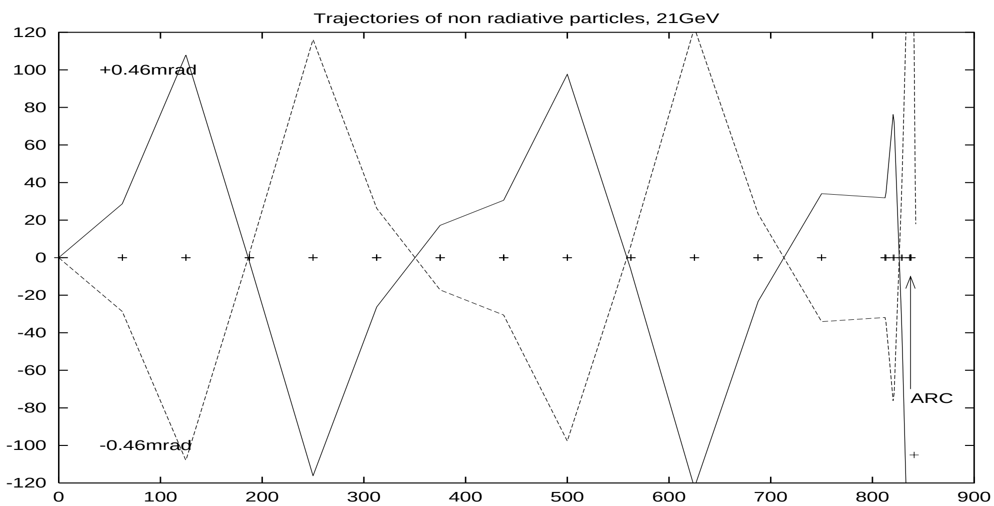

Figure 4: Trajectories in the horizontal plane of 21GeV non radiative particles crossing the straight section. The vertical range represents the acceptance of the straight section. The trajectories correspond to initial angles of 0.46mrad and zero amplitude, i.e. electrons emitted in the core of the muon beam.

The key point in the present discussion is the cut-off energy of the FODO cells. As they have a weak focusing, they can accommodate particles with a momentum down to 21GeV and a maximum acceptance. This is illustrated in figure (4). For instance particles with an energy of 19GeV and an initial angle corresponding to the acceptance of the section cannot pass through as shown on figure (5). For this case the maximum initial angle is 0.23mrad and consequently the fraction of particles passing with this energy is reduced by a factor of four compared with the particles at 21GeV. This fast decrease of the acceptance is explained by the fact that the FODO cells are unstable for an energy smaller than 18.4GeV. The phase

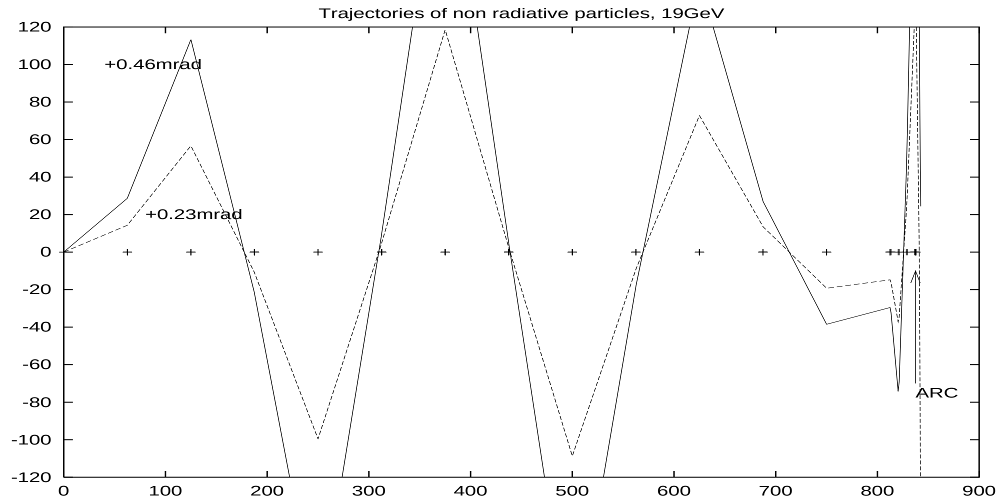

Figure 5: Trajectories in the horizontal plane of 19GeV non radiative particles crossing the straight section. The vertical range represents the acceptance of the straight section. The trajectory with an initial angles of 0.46mrad and zero amplitude hit the vacuum chamber. The with an initial angles of 0.23mrad and zero amplitude crosses the section

advance μ of a FODO cell of length L with the same integrated normalised gradient kl in both planes is :

$$\sin\frac{\mu}{2} = \frac{klL}{4}$$

The value of μ of the cells considered here is $2\pi \times 0.12$. It is clear that $\sin\frac{\mu}{2}$ remains smaller than 1 if k is multiplied by 2.7, i.e. if the particle momentum is divided by this number which gives 18.4GeV. Of course, for an energy just above this number, the phase advance is close to π and the β-functions are very large, which explains the above remark.

Although the electrons can propagate through the straight section with an energy of 21GeV, they may be lost in the matching section because of the off-momentum mismatch of this section. This is not considered here. A recent simulation shows that the energy loss in this section is appreciable [10].

3.2 Angular collection of the electrons crossing the straight section

Amplitude range/σ	0 / 0.5	0.5 / 1	1 / 1.5	1.5 / 2	2 / 2.5	2.5 / 3
Fraction of Gaussian	0.118	0.276	0.282	0.189	0.091	0.033
Max. angle/$10\gamma_\mu$	3	2.5	2	1.5	1	0.5
Min. angle/$10\gamma_\mu$	2.5	2	1.5	1	0.5	0

Table 1: Upper and lower limit of the angles of electrons passing through the straight section. The sum of the “fraction of Gaussian” is 0.99, i.e. a Gaussian distribution truncated at 3σ.

We assume that the muons have a Gaussian transverse distribution cut at 3σ by the machine acceptance. In order to evaluate the fraction of the electrons passing in this acceptance, the most simple procedure is to find out an upper and a lower limit of the emission angles at various amplitudes. To this end the muon distribution is split into six slices. The first slice concerns maximum amplitudes up to 0.5σ. An electron emitted by a muon with a 0.5σ amplitude can pass trough the section if its emission angle corresponds to 2.5σ if the muon trajectory has its maximum angle and a little more if it has a maximum amplitude. Thus for all muons with maximum amplitudes up to 0.5σ, the minimum collection angle is 2.5σ and the maximum obviously 3σ. For the slice of the muons distribution between 0.5σ and 1σ, the minimum angle corresponds to 2σ and the maximum to a little more than 2.5σ, and so on. This is summarised in table (1). The fraction of electron associated with each slice is then computed from the value of the solid angle they occupy the centre of mass. To this end formula (3) is equated to the collected angle given in table (1), that is rewritten x/γ_μ. We obtain:

$$x = \frac{\sin\theta}{1+\cos\theta} \tag{4}$$

the fraction of electrons emitted in the cone of angle θ being (1-cosθ)/2. We deduce that this fraction f_θ is eventually given by the simple expression :

$$f_\theta = \frac{x^2}{1+x^2} \tag{5}$$

Combining this with the numbers in table (1), we can compute that the upper limit of the fraction of electron passing through the straight section is 4.2% (it is somewhat underestimated because of the simplification done to build table (1)) and the lower limit is 2.6%. This is small but the electrons are produced all along the straight section which is 800m long at most and are lost in a region of the arc of much smaller length. This is examined now.

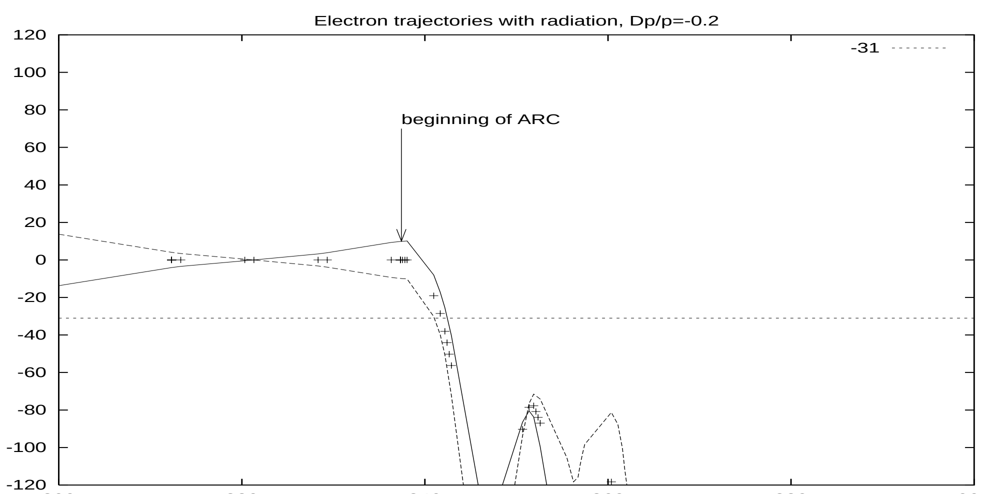

Figure 6: Trajectories in the horizontal plane of electrons emitted at the beginning of the straight section with a relative momentum deviation of -0.2, so that the on-axis trajectory touches the vacuum chamber at the end of the first quadrupole of the arc.

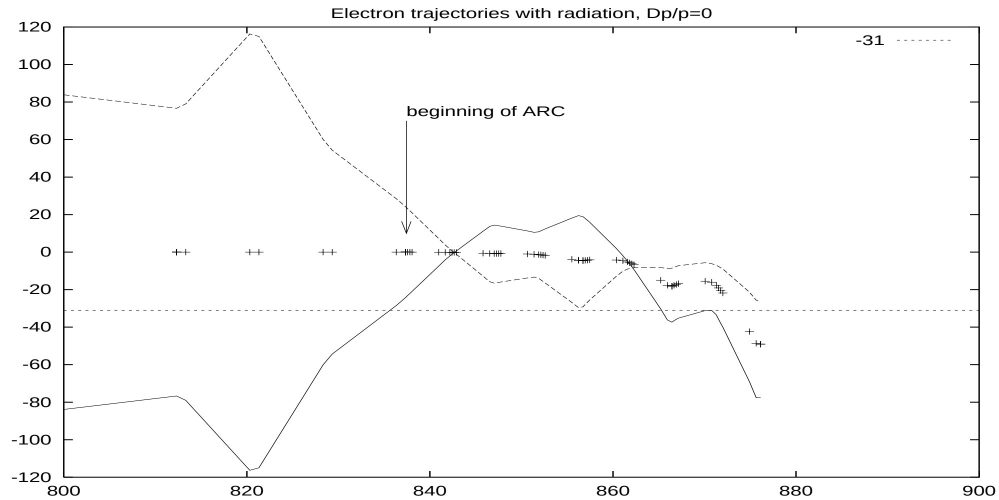

Figure 7: Trajectories in the horizontal plane of electrons emitted at the beginning of the straight section with an energy equal to that of the muons and no angle. It touches the vacuum chamber at the end of the first quadrupole of the arc.

4 Electrons reaching the arc

Tracking has been done to point out where the electrons emitted with a certain energy, which cross the straight section, arrive in the arc. The TWISS command in the MAD program with the radiate option has been used [11]. This guarantees a correct treatment of off-momentum trajectories. Trajectories have been tracked with different momentum deviations and zero initial slopes to identify in which element they touch the vacuum chamber in the arc, i.e. where their transverse horizontal coordinate becomes equal to -3σ=-31mm.

An example is shown on figure (6) of a trajectory in the arc with an initial large momentum deviation and a zero angle. For comparison A trajectory with only synchrotron radiation is shown on figure (7), it reaches the fifth dipole of the arc. In the extreme case of electrons of energy 21GeV, which can cross just the straight section with a 3σ angle, important losses occur in the matching section as can be seen on figure (8). This is not considered here.

The list of elements and associated momentum deviations is given in table (2).

5 Additional power dissipated in some arc elements

We are now in a position to compute the power carried by the electrons hitting the vacuum chamber of a given element. For each element it is possible to compute the momentum deviations δ_1 and δ_2 of two trajectories, one which hits its entrance and one which hits its exit. From these two values we can deduce the fraction f_δ of the electrons originating from the straight section hit this element, using the integral of differential distribution given by formula (1). As said above the variable x_i in this formula is equal to 1+δ_i. The value of f_δ is then given by :

$$2x_2^3 - x_2^4 - 2x_1^3 + x_1^4$$

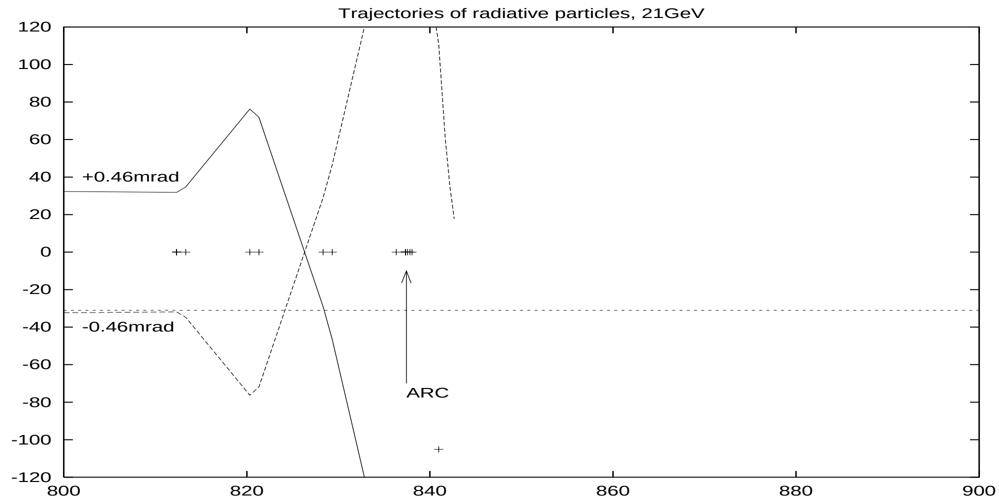

Figure 8: Trajectories in the horizontal plane of electrons emitted at the beginning of the straight section with an energy of 21GeV and no angle. It touches the vacuum chamber inside the first dipole of the arc. Trajectories with a large angle hit the vacuum chamber in the matching section.

The numbers associated with different elements in the arc are given in table (2).

The final power deposition is computed from the fraction of the power deposited in the straight section assuming that this fraction is small. The total power is $L_s P'$, L_s being the length of the straight section and P' the average deposited power. In what follows, we will take the value computed for the whole machine as an approximation, i.e. 133W/m. This power is associated with an average energy of 50/3GeV, then for the electrons under consideration, their power has to be scaled with their average energy $\bar{E}$. The fraction of the power dissipated in a given element is eventually given by :

$$L_s P' f_\delta f_\theta 3\bar{E}/50.$$

Alternatively we can define a loss addition factor A which is the ratio between the additional loss and the average one. For a value of L_s of 800m, we have :

$$A = 48\bar{E} f_\delta f_\theta$$

The values of A associated with the arc elements in which an additional loss occurs are listed in table (2).

6 Conclusion

A first crude estimation of the power deposited in the first magnets of the arc by the electrons originating from the muon decay in the straight section upstream of length 800m has been performed. The power deposited in the first elements of the arc is larger than the average deposited power by a factor between three and ten. Therefore a special attention has to be paid to the design of this magnets. Depending of the cooling possibilities it might be wise to use warm magnet or a permanent magnet at the beginning of the arc. Of course

element	L/m	δ_1	δ_2	$< E > /GeV$	f_δ	A	
1st dip.	2.91	-0.2915	-0.58	27	0.342	4.1	6.7
s. s.	0.72	-0.2155	-0.2915	37	0.127	1.6	2.5
1st QD	0.5	-0.1713	-0.2155	40	0.0797	1.8	2.8
str. sect.	0.24	-0.1520	-0.1713	42	0.0	7.9	12
1st sex.	0.24	-0.1360	-0.1520	43	0.0302	6.7	11
str. sect.	0.24	-0.1240	-0.1360	43.5	0.0229	5.2	8.3
2nd dip.	2.91	-0.0517	-0.1240	45.5	0.141	2.7	4.5
str. sect.	0.72	-0.0438	-0.0517	47.6	0.0157	1.3	2.1
1st QF	0.5	-0.0426	-0.0438	47.8	0.0024	0.3	0.46
3rd dip.	2.91	-0.0277	-0.0426	48.2	0.0377	0.78	1.3
str. sect.	0.72	-0.0209	-0.0277	48.8	0.0056	0.47	0.76
2nd QF	0.5	-0.0205	-0.0209	48.9	0.0008	0.10	0.16
4th dip.	2.91	-0.0127	-0.0205	49.2	0.0156	0.32	0.53
str. sect.	0.72	-0.0098	-0.0127	49.4	0.0058	0.49	0.8
3rd QF	0.5	-0.0093	-0.0098	49.5	0.0010	0.12	0.20
5th dip.	2.91	0.0	-0.0093	49.7	0.0186	0.40	0.64

Table 2: List of elements and associated momentum deviations. The values of the momentum deviations are such that a trajectory entering the arc with its value reach the end of the element. δ_1 and δ_2 are the relative momentum deviations respectively at the entrance and the exit of the element.

a more detailed study, e.g. a Monte Carlo simulation is necessary to evaluate precisely the power deposited in the magnets of the arc and the matching section. An example of such a calculation has been shown recently [10]. It should be pursued as the determination of the position of hot spots is of prime importance.

It is probably safe that the first quadrupole in the arc is an horizontal defocusing quadrupole as is the case in the present study. With a horizontal focusing quadrupole the power deposited must be larger because of the larger value of the dispersion function.

The mechanism described in this note should also be considered in the case of the muon collider. The electrons produced in the straight section upstream of the experiment are lost in the low-β quadrupoles and increase their heat load.

References

[1] A. Faugier, SPS statistics, private communication. Also SL-Note-99-051 OP.

[2] The LHC study group, The LARGE HADRON COLLIDER Conceptual design. CERN/AC/95-05(LHC), 20 October 1995.

[3] N. Mokhov, Beam induced energy deposition. FNAL collaboration meeting held in February 2000.

[4] F. Dydak, private communication.

[5] Particle Physics booklet (july 1998), page 234.

[6] J.B. Jeanneret and J. Pancin, Distribution of the electrons decaying from 50GeV muons. ν-factory note to be published.

[7] R.B. Palmer, C. Johnson and E. Keil, A cost-effective design for a neutrino factory. CERN SL/99-070 AP also Neutrino factory note 9 (November 1999).

[8] C. Johnstone and B. Autin, Large acceptance muon storage rings for neutrino production : lattice design. PAC New-york, March 1999.

[9] A. Verdier, Geometry of the muon storage ring. Neutrino factory note 13 (February 2000).

[10] E. Keil, Simulation of energy deposition in a muon storage ring. Meeting of the Neutrino Factory Working Group 22 March 2000.

[11] H. Grote and F.C. Iselin, The MAD program (Methodical Accelerator Design) version 8.16, User's reference manual, CERN/SL/90-13(AP), (rev. 4) (March 27, 1995).